Environmental Science & Technology

Article

pubs.acs.org/est

Eutrophication Increases Phytoplankton Methylmercury Concentrations in a Coastal Sea—A Baltic Sea Case Study

Anne. L. Soerensen,*[,†] Amina T. Schartup,[‡] Erik Gustafsson,[§] Bo G. Gustafsson,[§] Emma Undeman,[†,§] and Erik Björn[∥]

[†]Stockholm University, Department of Environmental Science and Analytical Chemistry, Stockholm SE-106 91, Sweden

[‡]Harvard University, John A. Paulson School of Engineering and Applied Sciences, Cambridge Massachusetts 02138, United States

[§]Stockholm University, Baltic Nest Institute, Baltic Sea Centre, Stockholm SE-106 91, Sweden

[∥]Umeå University, Department of Chemistry, Umeå SE-901 87, Sweden

Supporting Information

ABSTRACT: Eutrophication is expanding worldwide, but its implication for production and bioaccumulation of neurotoxic monomethylmercury (MeHg) is unknown. We developed a mercury (Hg) biogeochemical model for the Baltic Sea and used it to investigate the impact of eutrophication on phytoplankton MeHg concentrations. For model evaluation, we measured total methylated Hg ($MeHg_T$) in the Baltic Sea and found low concentrations (39 ± 16 fM) above the halocline and high concentrations in anoxic waters (1249 ± 369 fM). To close the Baltic Sea $MeHg_T$ budget, we inferred an average normoxic water column Hg^{II} methylation rate constant of 2×10^{-4} d^{-1}. We used the model to compare Baltic Sea's present-day (2005−2014) eutrophic state to an oligo/mesotrophic scenario. Eutrophication increases primary production and export of organic matter and associated Hg to the sediment effectively removing Hg from the active biogeochemical cycle; this results in a 27% lower present-day water column Hg reservoir. However, increase in organic matter production and remineralization stimulates microbial Hg methylation resulting in a seasonal increase in both water and phytoplankton MeHg reservoirs above the halocline. Previous studies of systems dominated by external MeHg sources or benthic production found eutrophication to decrease MeHg levels in plankton. This Baltic Sea study shows that in systems with MeHg production in the normoxic water column eutrophication can increase phytoplankton MeHg content.

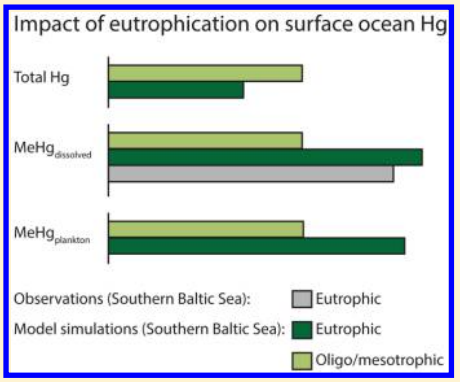

1. INTRODUCTION

Monomethylmercury (MeHg) is a neurotoxin that bioaccumulates in aquatic food webs.[1] Eutrophication in coastal areas and continental seas is expanding worldwide[2] potentially affecting MeHg production and its levels in food webs (e.g.,[3−5]). While many studies have investigated the role of eutrophication on isolated aspects of the mercury (Hg) cycle, its impact at the ecosystem level is uncertain.[3] Here we adapt an existing nutrient cycling model to include cycling of Hg species and phytoplankton accumulation of MeHg in the Baltic Sea, and use it to quantify the impact of eutrophication.

Eutrophication leads to greater net primary production, therefore increasing organic matter (OM) settling and decreasing light penetration. These in turn change redox conditions in water column and sediments.[6,7] The most comprehensive study on the impact of eutrophication on coastal marine Hg cycling[3] used a conceptual model to show that by increasing primary production eutrophication leads to a decrease in MeHg concentrations in biota. One important driver of this effect was proposed to be that the increase in phytoplankton biomass decreases the amount of MeHg in individual cells. This phenomenon, known as growth biodilution, has been observed in laboratory experiments[4] and in both marine and freshwater systems.[8−10] The conceptual model for coastal systems was based on earlier work that concluded that divalent inorganic mercury (Hg^{II}) methylation did not take place in normoxic (oxygen (O_2) > 2 mL L^{-1}) marine water columns.[11] However, several recent studies reported Hg^{II} methylation in normoxic waters,[12−14] possibly linked to the remineralization of organic matter.[15,16] Moreover, genes (*hgcAB*) coding for Hg^{II} methylation ability in microorganisms have been found in some normoxic and anoxic marine environments.[17,18] Therefore, the impact of eutrophication needs to be revisited using a model that includes in situ Hg^{II} methylation in the water column.

An increase in OM settling increases the biological oxygen demand. Severe eutrophication can result in bottom water hypoxia (<2 mL O_2 L^{-1}) or anoxia (lack of O_2).[2] In shallow freshwater systems, anoxia is usually correlated with elevated

Received: May 31, 2016
Revised: August 31, 2016
Accepted: October 5, 2016

DOI: 10.1021/acs.est.6b02717
Environ. Sci. Technol. XXXX, XXX, XXX−XXX

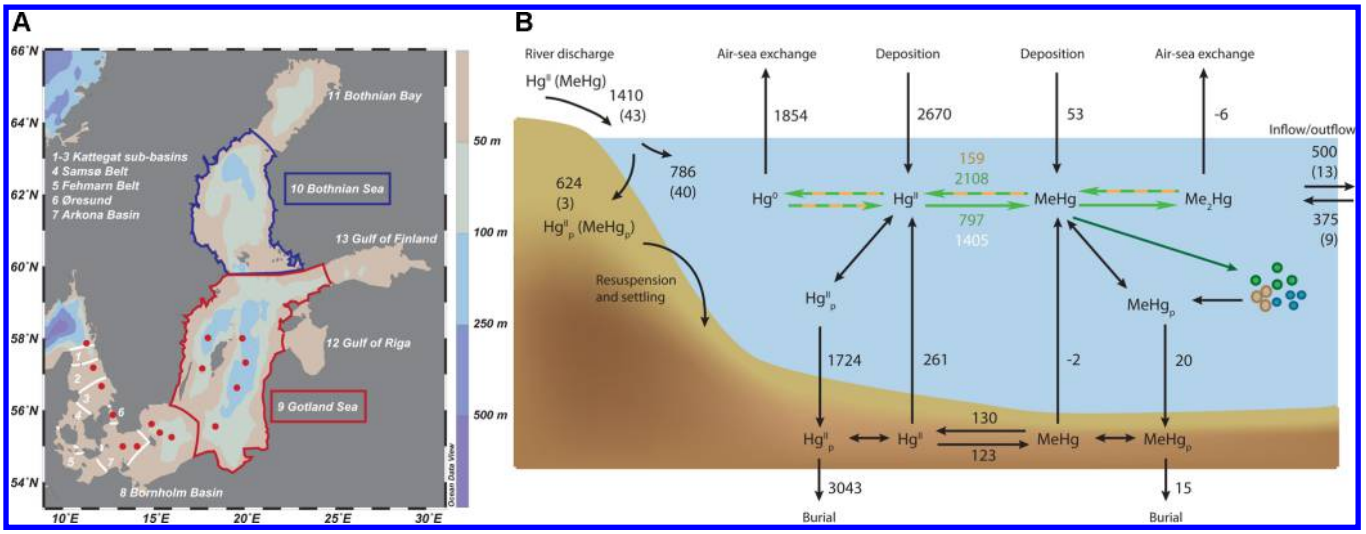

Figure 1. (A) The 13 basins in the Baltsem model and water column total methylated mercury ($MeHg_T$) sampling sites used for model evaluation (red circles). The Bothnian Sea (entirely normoxic water column) and the Gotland Sea (areas with hypoxic and anoxic water) are highlighted in blue and red, respectively. (B) Mass flow rates (kg y^{-1}) determined by the Baltsem-Hg simulation for all 13 Baltic Sea basins combined (2005−2014 average). (Striped) green arrows/text indicate biotically mediated water column mass flow rates in normoxic water, white text describes the methylation flow rate in the hypoxic/anoxic water column, (striped) orange arrows/text indicate photolytically mediated mass flow rates, and black arrows/text indicate other types of partitioning and rates. Numbers in parentheses are mass fluxes of MeHg (kg y^{-1}) in river discharge and Atlantic inflow/outflow.

MeHg levels.[19,20] The relationship has been explained by elevated diffusion of MeHg from sediment or in situ Hg^{II} methylation in anoxic waters.[20−22] High MeHg concentrations in bottom water can impact concentrations in surface waters through vertical mixing, advection, and convection.[5] Beutel et al.[19] found 50% higher MeHg levels in zooplankton in a freshwater lake during years with oxygen depletion and elevated MeHg concentration in bottom water. In seawater, Lamborg et al.[23] found elevated MeHg levels in the Black Sea's normoxic−anoxic water interface, where both dissolved oxygen and sulfide were low. The presence of anoxic areas in eutrophic estuarine and marine systems could increase MeHg concentrations in water and biota.

The Baltic Sea is semienclosed and divided into sub-basins by sills (Figure 1A). It is a shallow system (c.a. 50% less than 50 m deep),[24] with each sub-basin in a different stage of eutrophication.[25] Ventilation of the Baltic Sea's deep water layers through the shallow and narrow entrance area (Figure 1) is low and larger volumes of oxygen rich saltwater only enter irregularly (from years to decades[26]). The combination of stagnant periods in the deeper water layers and settling of OM elevated due to eutrophication results in areas with seasonal or permanent hypoxic and anoxic bottom waters.[27] Nitrogen (N) and phosphorus (P) inputs to the Baltic Sea peaked in the 1980s. A recent decline in inputs (15−20% between 1994 to 2010) did not result in lower nutrient concentrations in the open sea and anoxia in deep stagnant waters is still expanding.[25,28] Phytoplankton production is currently N limited, except for the production of N-fixating filamentous cyanobacteria that are P and temperature limited.[29]

Here we adapt a biogeochemical model developed to investigate the impact of eutrophication in the Baltic Sea to include Hg chemistry. To validate the model, we measure $MeHg_T$ (MeHg + dimethylmercury (Me_2Hg)) in 15 water profiles. We then use the model to investigate eutrophication-driven changes in Hg cycling and MeHg phytoplankton levels by comparing an oligo/mesotrophic scenario with a eutrophic (historic) scenario for the Baltic Sea.

2. METHODS

2.1. Data on Water Column Methylmercury and Incubation Experiments. To constrain MeHg processes and evaluate the model we collected water samples for $MeHg_T$ analysis during a cruise in the Southern Baltic Sea on the first to seventh September 2014 (Figure 1). The concentration of $MeHg_T$ in unfiltered samples was measured at 15 stations (2−8 depths). Twenty-one incubation experiments using enriched Hg isotope tracers were conducted in normoxic and anoxic water to determine Hg^{II} methylation and MeHg demethylation rate constants. We define the switch from hypoxic to anoxic conditions in the data set based on the presence of hydrogen sulfide (H_2S) in the water, which happened at <0.1 mL O_2 L^{-1} during the 2014 cruise. A detailed description of the sampling locations and methods are provided in the Supporting Information (text S1).

2.2. Model. Baltsem is a coupled physical−biogeochemical model that simulates eutrophication in the Baltic Sea.[28,30] The model divides the Baltic Sea into 13 interconnected sub-basins, each described as horizontally homogeneous but with a high vertical resolution (up to 250 layers/compartments) (Figure 1A; Figure S1). A sediment compartment also exists for each vertical layer and has an active depth of 1 cm (Figure S1). A hydrodynamic module simulates transport of state variables between and within basins.[31] The model simulates nutrient (N, P, Silica (Si)) and carbon cycling in the water column and sediment.[32] We add to the model four Hg species (Hg^{II}, gaseous elemental Hg (Hg^0), MeHg, and gaseous Me_2Hg) and phytoplankton bioaccumulation of MeHg (Figure 1B). Hg^{II} and MeHg are modeled as either dissolved (associated with ligands; <0.2 μm) or bound to particulate organic matter (POM; >0.2 μm) in the water column and sediment as described below. Details on model parametrizations are provided in Tables S3−S6.

DOI: 10.1021/acs.est.6b02717
Environ. Sci. Technol. XXXX, XXX, XXX−XXX

2.3. External Inputs—Present Day. River discharge of Hg^{II} is calculated from the total organic carbon (TOC) discharge[32] and a Hg:TOC ratio. For basins with large industrial catchments (Arkona Basin, Bornholm Basin, Gotland Sea, and Gulf of Gdansk) we use a ratio of 0.36 ng Hg per mg TOC measured in the Polish river Vistula that contributes 8% of the water discharge to the Baltic Sea.[33,34] Elsewhere, we use a ratio of 0.22 ng Hg per mg TOC based on observations from rivers across Sweden (R^2 = 0.4; p < 0.001, n = 3291).[35] We compare our basin specific river inputs of Hg^{II} to available observations in Table S1. Present day point sources are small (<2 kg y^{-1}) and included in HELCOM's river inventory.[36,37] We estimate an average riverine MeHg concentration of 415 fM using a correlation between observed $MeHg_T$ concentration and salinity in a Bothnian Bay estuary in 2015 (Figure S2). The sampling of water and $MeHg_T$ analysis followed the same method as in 2014 described in text S1.

To estimate the external input of particulate Hg from rivers, we use measured basin specific values for suspended solids in rivers and a partitioning coefficient for Hg^{II} (K_D = 10^5 L kg^{-1}; southern Baltic Sea rivers)[33,38] and MeHg (K_D = 10^4 L kg^{-1}). Globally, a large fraction of particulate Hg settles nearshore.[39] Two sediment dispersal systems from Walsh and Nittrouer[40] best represent the sediment dispersion in the Baltic Sea (estuarine accumulation dominated and proximal accumulation dominated). To best represent these systems, we force 85% of the particulate riverine Hg input to settle to sediments in the nearshore shallow area (<10m).

For atmospheric Hg^{II} deposition between 1990 and 2012, we distribute basin specific yearly deposition estimates from HELCOM to match the monthly variability.[41,42] We use the 2012 deposition estimate for 2013−2014. To estimate an atmospheric MeHg deposition, we use a MeHg fraction (g g^{-1}) of 2% of the deposited Hg^{II} based on measurements in Sweden and elsewhere.[43−45]

Hg^{II} concentrations (1 pM) and Hg^0 concentrations (100 fM) in Atlantic Ocean inflow water are taken from measurements below the thermocline at Samsø Belt,[46] and measurements in the southern Baltic Sea, respectively.[47,48] MeHg concentrations (25 fM) in Atlantic inflow water are from our most northern station in the Kattegat sub-basins (Figure 1) and Me_2Hg (5 fM) is based on measurements in the Mediterranean Sea.[49] The concentrations of all Hg species in inflow water are kept constant during the simulations.

2.4. External Inputs—1850 to Present. We use historic information on changes in Hg concentrations in river water discharge (1985−2013)[35,50] and Hg concentrations in sediment cores (1850−2000)[51] to scale the Hg:TOC ratio between 1850 and present (for details, see text S2). To obtain a pre-1990 precipitation estimate we use the relative change in global Hg deposition from Horowitz et al.[52] to scale the changes in atmospheric Hg deposition in the Baltic Sea.

2.5. Water Chemistry. At each time step (3 h), we calculate the fraction of Hg^{II} and MeHg in the dissolved phase and the fraction sorbed to POM using partitioning coefficients (Hg^{II}: K_D = 10^5 L kg^{-1}; MeHg: K_D = 10^4 L kg^{-1})[53] (Table S3).

Schartup et al.[54] suggests that the presence of terrestrial dissolved organic matter (TDOM) decreases the reducible fraction of dissolved Hg^{II}. Soerensen et al.[55] found that for the open ocean a modeled reducible fraction of dissolved Hg^{II} of 40% best matched observations. The offshore fraction of TDOM increases from south to north in the Baltic Sea.[56] We estimate a TDOM dependent reducible reservoir of dissolved Hg^{II} (see Table S4)[54,57] that ranges from 35% in Kattegat to 10−15% in the Bothnian Bay.

We use Hg redox transformation rate constants (photolytic reduction and oxidation, biotic reduction and dark oxidation) from Soerensen et al.[55] We scale the biotic Hg^{II} reduction rate constant using the remineralization rate (Table S4).

A range of factors, such as the concentration of chloride ions, and the dissolved organic matter (DOM) quality and concentration, influences photodemethylation.[58−60] We use observed variability in demethylation seen across salinity gradients to scale the photodemethylation rate constant (k_{pdem}: PAR × (−0.027 × salinity + 1); Table S4).[60,61] Temporal and spatial variability in light attenuation is taken into account.[30] The dark demethylation rate constant is set based on the average in our incubation experiments (k_{bdem}: 0.04 d^{-1}; Text S1). Jonsson et al.[62] found that up to 30% of MeHg bound to terrestrial OM was not readily available for dark demethylation. We assume that MeHg bound to TDOM is less available than MeHg bound to marine DOM. This result in a MeHg fraction available for biotic demethylation that increases as the TDOM concentration decreases from the Bothnian Bay (40% available) to Kattegat (70% available) (Figure 1A; Table S4).

We did not measure any Hg^{II} methylation rate constants above the detection limit (DL: 4 × 10^{-4} d^{-1}) during the 2014 September cruise (see section 3.1). However, based on dark demethylation rate constants from the cruise and use of calculated upper boundaries on MeHg sources other than Hg^{II} methylation (river, deposition, and sediment diffusion), we cannot reproduce the measured $MeHg_T$ concentrations without including water column Hg^{II} methylation. In normoxic waters, in situ methylation (<40 × 10^{-4} d^{-1}) has recently been measured in subarctic and midlatitude estuarine and coastal environments.[12,14] For the normoxic water column, we therefore use a low Hg^{II} methylation rate constant scaled to the remineralization rate of autochthonous POM[15] that on average is 50% of the field campaign detection limit (average rate used: 2 × 10^{-4} d^{-1}). Eckley and Hintelmann[21] found Hg^{II} methylation rates from < DL to 0.15 d^{-1} in some anoxic lake waters. We infer a methylation rate constant in oxygen-depleted water in order to match observed $MeHg_T$ concentrations in 2014. On the basis of a significant correlation between $MeHg_T$ and PO_4^{3-} observed in oxygen-depleted water during our cruise (R^2 = 0.83, P < 0.001, n = 17) we scale the Hg^{II} methylation rate by PO_4^{3-} concentrations (max of 0.015 d^{-1}; Table S4).

For Me_2Hg production and biotic and photolytic decomposition we follow Soerensen et al.[63] but modify the rates for middle latitude conditions where the Me_2Hg:MeHg ratio is lower than in the Arctic surface waters (Table S4).

2.6. Phytoplankton Bioaccumulation. We calculate the bioaccumulation of MeHg into phytoplankton. Hammerschmidt et al.[8] observed that the bioaccumulation factor (BAF) changed with autochthonous POM concentration (mPOM) on the continental margin of the Atlantic Ocean. This is supported by estuarine observations by Schartup et al.[12] We use data from the two papers to develop a mPOM-BAF relationship (Figure S3):

$$\log(\mathrm{BAF}) = 5 - \mathrm{mPOM} \quad (\text{for mPOM} < 1)$$

$$\log(\mathrm{BAF}) = 4.3 - 0.3 \times \mathrm{mPOM} \quad (\text{for mPOM} > 1)$$

where BAF is in L kg^{-1} wet weight and mPOM is in mg L^{-1}.

DOI: 10.1021/acs.est.6b02717
Environ. Sci. Technol. XXXX, XXX, XXX−XXX

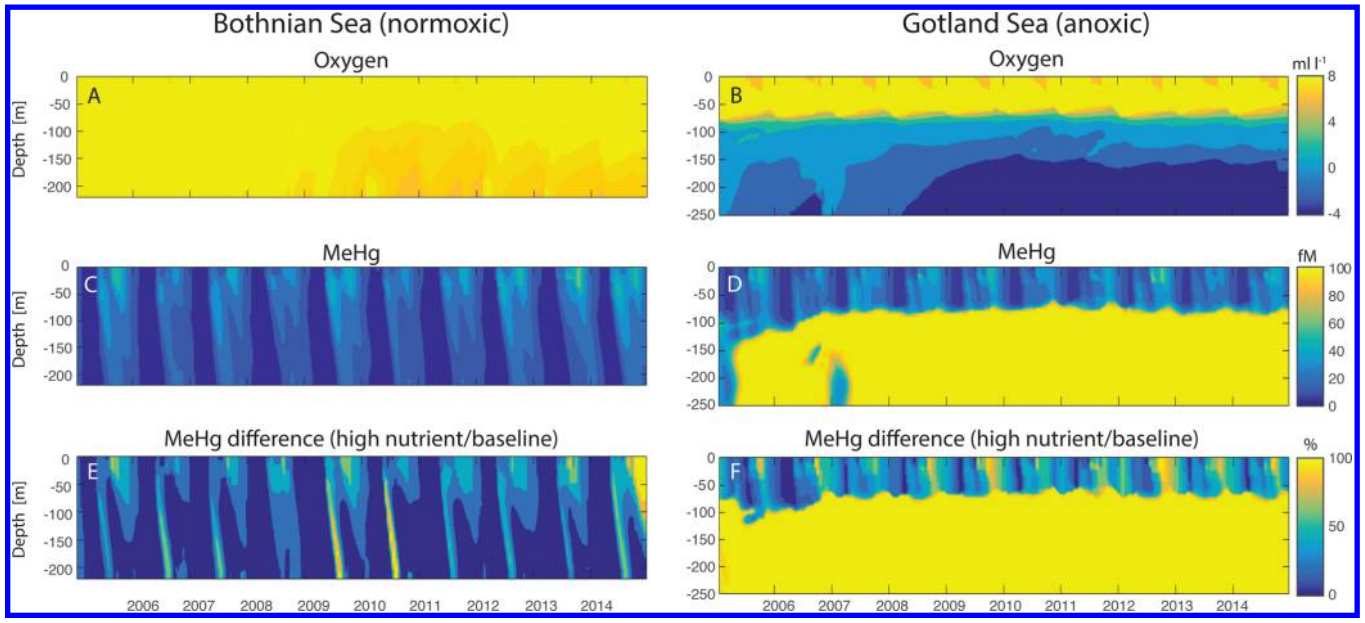

Figure 2. Concentration of oxygen (A+B) and monomethylmercury (MeHg; C+D) in the Bothnian Sea and the Gotland Sea (2005−2014) for the high (historical) nutrient scenario. E+F show the percent increase in MeHg concentration between the baseline and high nutrient scenarios. For D and F, the scale is capped at 100 fM and 100%, respectively, so that seasonal variability in surface water is visible. The effect of saltwater inflow events is visible in the bottom water oxygen (B) and MeHg (D) concentrations in 2005 and 2007.

2.7. Sediment Chemistry and Diffusion. Partitioning coefficients are used to calculate the fraction of sediment Hg found in pore water. We use the linear correlation between sediment OM content (%loss on ignition) and Hg_T and $MeHg_T$ observed by Hollweg et al.[64] to describe the variability of the sediment partitioning coefficients (K_D) with changing OM content (Table S5). For the Gotland Sea and the Bothnian Sea, the Hg^{II} K_D range is $10^{5.0-5.5}$ and $10^{4.0-4.5}$ and the MeHg K_D range is $10^{4.0-4.5}$ and $10^{3.0-3.5}$, respectively.

The sediment methylation rate constant (0.03 d^{-1}) for pore water Hg^{II} is taken from midlatitude estuarine and shelf regions[64,65] and the demethylation rate (4 d^{-1}) from the Atlantic Ocean shelf (4 ± 3 d^{-1}).[64] We validate these rates by comparing the model $MeHg_T$:Hg_T sediment ratio to present day data for the Baltic Sea (~0.2%).[51,66]

Diffusion rates of dissolved Hg^{II} and MeHg from sediment to the overlaying water is calculated using a diffusive transport equation based on Fick's law (Table S5). We differentiate between sediment with a thin oxygenated surface layer and fully anoxic sediment. For sediment with an oxygenated surface layer, we assume that all Hg is bound to thiols, while in fully anoxic sediment, we assume that all Hg is bound to inorganic sulfide species ($Hg(SH)_2$; HgS_2H^-; CH_3HgSH; CH_3HgS^-). This assumption is based on 1) observations that show that dissolved sulfides are rapidly depleted at oxygenated conditions while thiol compounds can persist,[67] and 2) that anoxic sediment in the Baltic Sea has dissolved sulfide concentrations high enough for dissolved Hg species to bind exclusively with sulfide rather than thiols.[68] Diffusivity rates for these complexes are from Hollweg et al.:[64] 2×10^{-6} cm^2 s^{-1} (thiol-bound Hg) and 10×10^{-6} cm^2 s^{-1} (Hg species with inorganic sulfide), respectively.

Resuspension in the Baltsem model is described as a lateral movement of sediment along the sea floor toward deeper areas[30] that does not result in sediment associated Hg being released to the water column. This transport captures the net effect of lateral resuspension over time but not short-term vertical resuspension and resettling dynamics. This could result in an underestimation of the Hg vertical resuspension flux, but our parametrization is consistent with prior studies in estuarine systems where vertical Hg resuspension is small compared to other water column sources.[12,69] An increase in OM sedimentation to the sea-floor leads to a quicker sediment burial,[70] and we link the Hg burial rate to OM sedimentation rate (Table S5).

2.8. Losses to External Reservoirs. Evasion of Hg^0 and Me_2Hg across the air−sea interface is based on the concentration gradient between the surface water and boundary layer gas concentration using the Nightingale et al.[71] parametrization for averaged wind speeds (Table S6). Small variations in atmospheric Hg concentrations have little impact on air−sea exchange.[57] We therefore use yearly average air concentrations and scale historic changes in atmospheric Hg^0 over the Baltic Sea to the global changes presented in Horowitz et al.[52] We maintain a constant Me_2Hg air concentration of 4 pg m^{-3}.[72]

2.9. Simulated Scenarios. In order to explore the effect of eutrophication we focus on average results from the Baltic Sea as well as two sub-basins: the Bothnian Sea and the Gotland Sea (Figure 1). Both sub-basins have experienced elevated nutrient inputs in the last century,[28] but differ in their bottom water oxygen levels. A strong stratification at the halocline (~60 m) efficiently suppresses vertical exchange between surface waters and deeper water masses most of the year in the Gotland Sea. As a result, the Gotland Sea often develops areas with hypoxia, including anoxia, in the deep stagnant water layers below the permanent halocline[73] while the Bothnian Sea has an entirely normoxic water column (Figure 2). We run two model scenarios. A baseline scenario where nutrient loads are kept constant at the 1920 level from 1920 to 2014 represents an unimpacted system while a "high nutrient" scenario with 20th century nutrient loads to the Baltic Sea represents present day conditions.[28] On average the "high nutrient" scenario has a 100% higher N and P input from 1920 to 2004 and 236% and

DOI: 10.1021/acs.est.6b02717
Environ. Sci. Technol. XXXX, XXX, XXX−XXX

Table 1. Total Mercury (Hg_T), Total Methylated Mercury ($MeHg_T$), and Other Variables in Water Column and Sediment Reservoirs[a]

	Baltic Sea			Bothnian Sea (normoxic)			Gotland Sea (anoxic)		
	baseline	high nutrient	high:base	baseline	high nutrient	high:base	baseline	high nutrient	high:base
$Hg_{T\text{-}aq}$ (Mg)	9.5	7.0	0.7	2.2	1.6	0.7	4.4	3.1	0.7
$MeHg_{T\text{-}aq}$ (Mg × 10^3)	72	284	4.0	13	18	1.4	35	228	5.8
Hg_{sed} (Mg)	101	93	0.9	16	19	1.2	40	35	0.9
$MeHg_{sed}$ (Mg)	0.17	0.41	2.4	0.02	0.04	2.0	0.07	0.22	3.1
N (Mg × 10^3)	655	976	1.5	83	187	2.3	404	421	1.0
P (Mg × 10^3)	247	540	2.2	26	55	2.1	180	402	2.2
$N_{plankton}$ (Mg × 10^3)	6	15	2.5	0.6	1.5	2.5	2.8	6.3	2.3
water (m^3)	21.6 × 10^{12}			11.7 × 10^{12}			4.3 × 10^{12}		

[a]The difference is calculated as the fraction of high nutrient:baseline scenario.

250% higher N and P loads from 2005 to 2014 compared to the baseline scenario (Figure S4). We explore the difference in Hg dynamics between the two scenarios for the period 2005−2014 during which the changes in external Hg inputs are minimal.

3. RESULTS AND DISCUSSION

3.1. Observed $MeHg_T$ Concentrations and Hg Rate Constants. The spatial distribution of $MeHg_T$ concentrations is presented in Figure S5. We find low $MeHg_T$ concentrations (39 ± 16 fM, n = 41) above the permanent halocline (60 m) across the southern Baltic Basins. $MeHg_T$ concentrations are up to 42 times higher in the low oxygen water masses of the Gotland Sea; a maximum of 510 fM (217 ± 209 fM) in hypoxic water and of 1640 fM in anoxic water (1249 ± 369 fM). In hypoxic and anoxic water, we find a significant correlation between $MeHg_T$ and PO_4^{3-} (R^2 = 0.83, P < 0.001, n = 17). This suggests that MeHg production is related to microbial remineralization of OM in the O_2 depleted water column.[74,75]

Hg^{II} methylation rate constants were all below the detection limit (4 × 10^{-4} d^{-1}). MeHg dark demethylation rate constants ranged from below the detection limit (0.03 d^{-1}) to 0.17 d^{-1} (52% of the rates constants were above the detection limit). MeHg dark demethylation rate constants were not correlated to measured auxiliary parameters.

3.2. Model Comparison to Observations. Figure S6 shows a comparison between modeled data and observations (observations are averaged across basins and 10−20 m depth intervals) in selected basins. Hg species measurements were collected in the southern part of the Baltic Sea. We use this data to validate the model and evaluate processes across the entire system. We find a significant correlation (R^2 = 0.64, P < 0.01, n = 39) between measured and modeled concentration of water column $MeHg_T$. Modeled and measured Hg_T concentrations (HELCOM 2006−2009 averages)[46] are weakly correlated (R^2 = 0.1, P < 0.1, n = 28) and 97% of modeled Hg_T concentrations are within one standard deviation of observed values. The monthly variability of Hg^0 is well captured by the model (R^2 = 0.68, P < 0.1, n = 5; Figure S7).[47,48] Modeled concentrations of Hg_T in sediment cores reproduce the measured historic sediment total Hg concentrations between 1850 and 2000 in the Gotland Sea (R^2 = 0.70, P < 0.01, n = 18), Bothnian Bay (R^2 = 0.85, P < 0.01, n = 18), and Gulf of Finland (R^2 = 0.63, P < 0.01, n = 23) (observations from Leipe et al.)[51] For present day, 63% of Hg_T sediment observations are within one standard deviation of observations (n = 31) (Figure S8).

3.3. Present Day Baltic Sea Budget. We find a total reservoir of 7.4 Mg Hg in the Baltic Sea water column, 4% of which is in the form of $MeHg_T$ (Table 1B). Figure 1 shows external inputs and internal mass flow rates of Hg species for the Baltic Sea. The main sources of Hg are atmospheric deposition (60%) and river discharge (32%; of which 43% deposits close to the river mouth) while inflow from the North Sea is small (8%). Hg is lost through burial (56% of total loss), evasion (34%), and outflow (10%). It has been suggested that the Baltic Sea is a net source of Hg to the atmosphere[47] but by combining all available data into our model framework we update this estimate. We find that the Baltic Sea is a net sink for atmospheric Hg and that the evasion loss is 32% (0.9 Mg y^{-1}) smaller than input through deposition (Figure 1). However, due to high historic Hg inputs that are now stored in the sediment (Figure S4) the active reservoirs in the Baltic Sea (water and 1 cm surface sediment) are currently reduced by 0.8 Mg y^{-1}, which is approximately 1% of the Hg_T reservoir (Table 1). This loss is driven by burial of Hg bound to OM into deeper inactive sediment layers, as new material settles to the sea floor. External MeHg inputs from rivers and deposition are comparable, but river inputs could have a more pronounced effect close to river mouths where the river water MeHg concentrations have not yet been significantly diluted. Sediment diffusion is not a significant source of MeHg to the overlaying water as also shown for other systems,[12,69,76] although this flux could be slightly underestimated as the effect of sediment vertical resuspension is not included. We find that there is a net internal loss (net demethylation) of $MeHg_T$ (0.07 Mg y^{-1}) within the system.

3.4. Impacts of Eutrophication on Total Hg Dynamics. Table 1 presents the response of Hg_T, $MeHg_T$, and nutrient reservoirs to the two scenarios. We observe a 27% decrease in the Hg water reservoir size in response to increased eutrophication (high nutrient scenario). This decrease occurs in both the normoxic and anoxic basins and is due to a 37−50% increase in particle settling rate and a >90% decrease in diffusion from sediments. Eutrophication increases primary production leading to increased particle settling and Hg scavenging. Particle settling also increases sediment OM content resulting in an increased partitioning of sediment Hg to the solid phase, thereby lowering pore water Hg and diffusion into the overlaying water. Hg removal associated with particle settling out of the upper water column also results in a 30−40% lower Hg evasion; however, the increased loss rate to sediment is larger and therefore drives an overall decline in water column Hg. We find that the Baltic Sea under a low nutrient baseline regime is close to equilibrium between Hg deposition and evasion, but becomes a sink for atmospheric Hg under the high nutrient scenario as it is the case today with 32% of atmospheric deposition retained. We suggest that decreasing

DOI: 10.1021/acs.est.6b02717
Environ. Sci. Technol. XXXX, XXX, XXX−XXX

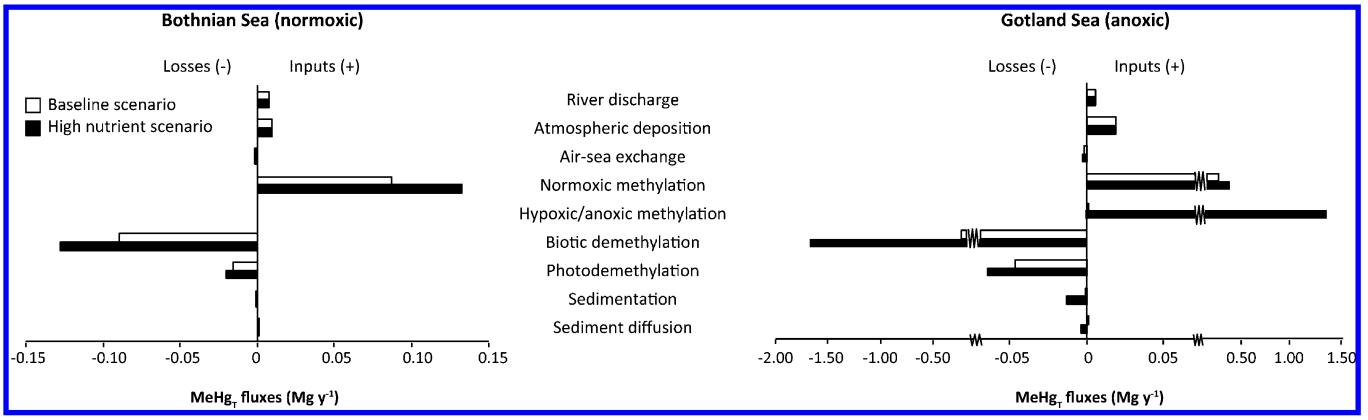

Figure 3. Average 2005−2014 inputs and losses for total methylated mercury ($MeHg_T$) reservoirs (Mg y^{-1}). The difference between baseline (white bars) and high nutrient scenarios (black bars) represents the effect of eutrophication on individual $MeHg_T$ fluxes. Note the change in scale for the Gotland Sea.

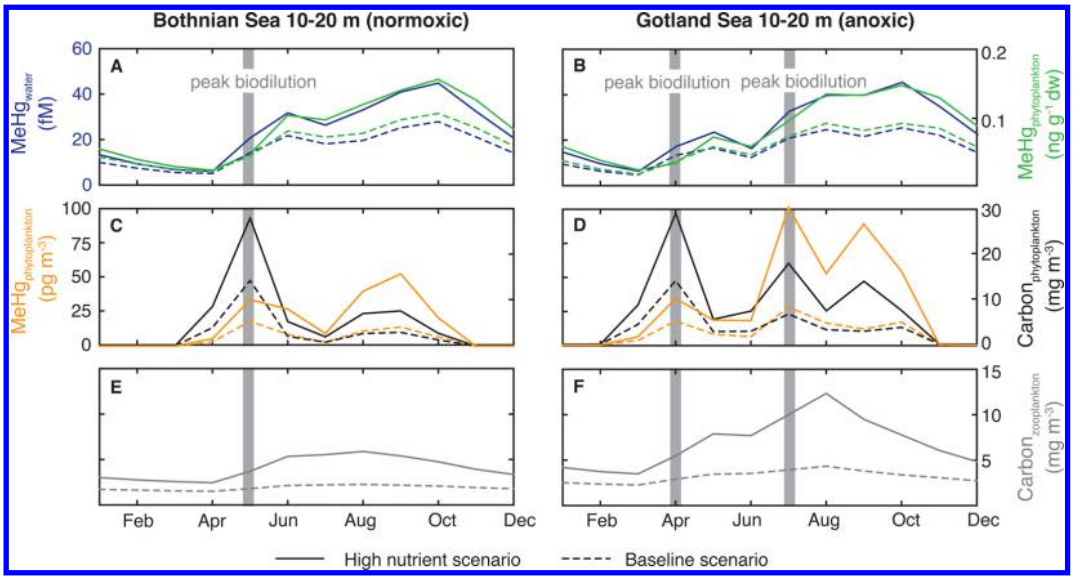

Figure 4. Seasonal variability (2005−2014) of (A, B) water column concentrations and phytoplankton monomethylmercury (MeHg) content, (C, D) phytoplankton MeHg and carbon volume concentrations and (E, F) zooplankton carbon volume concentrations. Solid lines represent the high nutrient scenario, dashed lines the baseline scenario. Gray bars indicate periods with particularly strong phytoplankton growth biodilution.

nutrient loads to coastal systems and closed seas in an effort to combat eutrophication will reduce the fraction of atmospheric Hg retained by the system through burial in inactive sediments. This will increase the lifetime of Hg in active biogeochemical cycling.

3.5. Basin-Wide Impacts of Eutrophication on MeHg Dynamics. Despite the large decrease in the Hg^{II} reservoir, the Baltic Sea water column $MeHg_T$ reservoir is on average 4 times higher under the high nutrient regime (Table 1). In basins with anoxic bottom water, the effect is larger (500% increase in Gotland Sea average $MeHg_T$ concentration) than in normoxic basins (38% increase in the Bothnian Sea). Only about 10% of the Baltic Sea total volume turns hypoxic and anoxic,[27] but the 10−80 fold increase in $MeHg_T$ concentrations in these waters is enough to drive a large average increase of the entire $MeHg_T$ reservoir (Figure 2).

Figure 3 contrasts the response of $MeHg_T$ mass flow rates to the baseline and high nutrient scenarios in normoxic and anoxic systems. We find that photolytic demethylation increases 40% in response to eutrophication in our scenarios (Figure 3). While eutrophication reduces the MeHg photodemethylation rate constants by increasing light attenuation, the simultaneous increase in the water column $MeHg_T$ reservoir results in an overall increase in MeHg photodemethylation rates.

In the high nutrient scenario Hg^{II} methylation and MeHg demethylation rates increase in both basins. However, methylation increases more resulting in an increase in the $MeHg_T$ reservoir sizes. Previous studies on the impact of eutrophication have focused on lakes and coastal estuarine systems where in situ Hg^{II} methylation in normoxic water has been considered nonexistent/negligible compared to other sources.[3] A synthesis of these studies indicated that eutrophication decreased the $MeHg_T$ reservoir.[3] We find that in the Baltic Sea the presence of even a low rate of water column Hg^{II} methylation can change the impact of eutrophication on water column MeHg concentrations. This suggests that other systems with water column Hg^{II} methylation could also see higher MeHg levels in response to increased eutrophication, unlike in previously studied systems where the MeHg water reservoir size is driven by external or benthic sources of MeHg.

DOI: 10.1021/acs.est.6b02717
Environ. Sci. Technol. XXXX, XXX, XXX−XXX

3.6. Seasonal Variability in MeHg Concentration. Figure 4 explores the impact of eutrophication on seasonal MeHg concentrations in surface water and phytoplankton. The model simulation suggests that the MeHg water concentration is lowest during winter and early spring but starts increasing at the end of the spring phytoplankton bloom coinciding with remineralization of dead plankton biomass (April−May). The MeHg concentration continues to increase through summer and peaks in fall (September−October). Phytoplankton MeHg content (ng g^{-1}) closely follows the change in water MeHg concentration. A peak biodilution effect on MeHg content, most pronounced for the high nutrient scenario, is observed during phytoplankton blooms (Bothnian Sea: May, Gotland Sea: April and July; indicated with gray bars on Figure 4). During these blooms increases in water MeHg concentrations in the high nutrient scenario do not drive a proportional increase in phytoplankton MeHg content (Figure 4A,B).

The volume concentration of MeHg in phytoplankton (pg m^{-3}) is positively correlated to both phytoplankton biomass (represented as carbon content on Figure 4C,D) and water MeHg concentrations. Despite the larger biomass of the spring phytoplankton bloom, highest phytoplankton MeHg volume concentrations are predicted for summer and fall bloom when water MeHg is highest (Figure 4C,D).

3.7. Impacts of Eutrophication on Surface Layer MeHg Dynamics. Methylmercury surface water concentrations in normoxic and anoxic basins respond similarly to increased eutrophication (44% and 53% increase, respectively) despite the uneven changes in the basin wide MeHg reservoir sizes (38% and 500%, respectively; Figure 4; Table S2). Winter surface cooling results in periodic vertical mixing of water across the halocline as observed for both P and methane.[26,77] In the Gotland Sea (anoxic) high MeHg concentrations below the halocline could be a source of MeHg to the surface layer (Figure 2). However, we find little difference in surface water MeHg winter concentrations between scenarios in the anoxic basin. This suggests that MeHg is demethylated faster at the surface than it is replenished from the subsurface. We conclude that the halocline effectively separates the MeHg reservoirs above and below it (Figure 4). When bottom water becomes anoxic, large quantities of P are released from the sediment and some of it reaches the surface water in winter through vertical transport.[26] This P promotes increased summer biomass by boosting net primary production of N-fixing cyanobacteria.[78] This is not seen to the same extent in basins with entirely normoxic water columns like the Bothnian Sea. An indirect effect of anoxic conditions in the Gotland Sea may be an increase in the phytoplankton bound MeHg reservoir (pg m^{-3}) available for zooplankton consumption in summer.

While surface water MeHg concentrations increase 44% and 53% in the Bothnian Sea and Gotland Sea, phytoplankton MeHg content increases only 33% and 46% between the baseline and the high nutrient scenario, respectively (Table S2). This suggests that there is a modest effect of growth biodilution between MeHg in water column and in phytoplankton at the ecosystem scale. However, eutrophication leads to higher biodilution during the spring bloom (May for the Bothnian Sea and April for the Gotland Sea) resulting in a 30−35% decrease in the transfer of water MeHg to phytoplankton (Figure 4A,B green to blue line ratio). This agrees qualitatively with previous findings of an 80% decrease in phytoplankton MeHg content across an increasing eutrophication gradient in a freshwater mesocosm study[9] and a 70% drop in phytoplankton MeHg content during an algal bloom in a coastal estuary.[4] We conclude that there can be pronounced seasonal and spatial impacts of biodilution as a system becomes more eutrophic but we find no evidence that eutrophication leads to a large system-wide decrease in MeHg phytoplankton content when averaged over a year.

We find the largest increase in water and phytoplankton MeHg between the baseline and high nutrient scenario in summer and fall (60−70% increase in phytoplankton MeHg content (ng g^{-1}) compared to a yearly average of 30−50%). This is driven by remineralization of dead plankton biomass from the spring and summer blooms that results in high in situ methylation followed by uptake into phytoplankton. The transfer of MeHg further up the food web depends on the seasonal variability of phytoplankton MeHg content, the quality of the phytoplankton community as a food source, and the timing of peak zooplankton grazing. Filamentous cyanobacteria make up a large fraction of Gotland Sea phytoplankton blooms.[29] The direct contribution of this phytoplankton fraction to secondary producers has been debated but new studies suggest that cyanobacteria are a better energy (and therefore likely MeHg) source for zooplankton than previously thought.[79−81] Furthermore, we find that the peak impact of eutrophication on phytoplankton MeHg content (ng g^{-1}) coincides with highest zooplankton grazing (biomass) (Figure 4G,H). Thus, eutrophication has the potential to enhance the transfer of MeHg not only to phytoplankton but also to higher trophic levels.

■ ASSOCIATED CONTENT

Supporting Information

The Supporting Information is available free of charge on the ACS Publications website at DOI: 10.1021/acs.est.6b02717.

Additional information includes cruise methods and description of model parametrizations (PDF)

■ AUTHOR INFORMATION

Corresponding Author

*Phone: +46 86747278; e-mail: anne.soerensen@aces.su.se.

Notes

The authors declare no competing financial interest.

■ ACKNOWLEDGMENTS

We acknowledge funding from the Danish Council for Independent Research (grants 1325-00030 and 1323-00745), the Swedish Research Council Formas (grant 2014-1088) and the Kempe Foundation (grant SMK-1243). We thank the Swedish Meteorological and Hydrological Institute and chief scientist Martin Hansson for letting us participate on their research cruise with R/V Aranda and Lars Lambertsson for help in the laboratory. We thank Lars-Eric Heimbürger for helpful discussions. Development of Baltsem is a part of the core activities of the Baltic Nest Institute supported by the Swedish Agency for Marine and Water Management.

■ REFERENCES

(1) Lavoie, R. A.; Jardine, T. D.; Chumchal, M. M.; Kidd, K. A.; Campbell, L. M. Biomagnification of Mercury in Aquatic Food Webs: A Worldwide Meta-Analysis. *Environ. Sci. Technol.* **2013**, *47* (23), 13385−13394.

(2) Diaz, R. J.; Rosenberg, R. Spreading Dead Zones and Consequences for Marine Ecosystems. *Science* **2008**, *321*, 926−929.

DOI: 10.1021/acs.est.6b02717
Environ. Sci. Technol. XXXX, XXX, XXX−XXX

(3) Driscoll, C. T.; Chen, C. Y.; Hammerschmidt, C. R.; Mason, R. P.; Gilmour, C. C.; Sunderland, E. M.; Greenfield, B. K.; Buckman, K. L.; Lamborg, C. H. Nutrient Supply and Mercury Dynamics in Marine Ecosystems: A Conceptual Model. *Environ. Res.* **2012**, *119*, 118−131.
(4) Luengen, A. C.; Russell Flegal, A. Role of Phytoplankton in Mercury Cycling in the San Francisco Bay Estuary. *Limnol. Oceanogr.* **2009**, *54* (1), 23−40.
(5) Todorova, S. G.; Driscoll, C. T.; Effler, S. W.; O'Donnell, S.; Matthews, D. A.; Todorov, D. L.; Gindlesperger, S. Changes in the Long-Term Supply of Mercury Species to the Upper Mixed Waters of a Recovering Lake. *Environ. Pollut.* **2014**, *185*, 314−321.
(6) Capriulo, G.; Smith, G.; Troy, R.; Wikfors, G.; Pellet, J.; Yarish, C. The Planktonic Food Web Structure of a Temperate Zone Estuary, and Its Alteration Due to Eutrophication. In *Nutrients and Eutrophication in Estuaries and Coastal Waters*; Springer: New York, 2002; pp 263−333.
(7) Karlson, K.; Rosenberg, R.; Bondsdorff, E. Temporal and Spatial Large-Scale Effects of Eutrophication and Oxygen Deficiency on Benthic Fauna in Scandinavian and Baltic Waters: A Review. *Oceanogr. Mar. Biol.* **2002**, *40*, 427−489.
(8) Hammerschmidt, C. R.; Finiguerra, M. B.; Weller, R. L.; Fitzgerald, W. F. Methylmercury Accumulation in Plankton on the Continental Margin of the Northwest Atlantic Ocean. *Environ. Sci. Technol.* **2013**, *47* (8), 3671−3677.
(9) Pickhardt, P. C.; Folt, C. L.; Chen, C. Y.; Klaue, B.; Blum, J. D. Algal Blooms Reduce the Uptake of Toxic Methylmercury in Freshwater Food Webs. *Proc. Natl. Acad. Sci. U. S. A.* **2002**, *99* (7), 4419−4423.
(10) Chen, C. Y.; Folt, C. L. High Plankton Densities Reduce Mercury Biomagnification. *Environ. Sci. Technol.* **2005**, *39* (1), 115−121.
(11) Whalin, L.; Kim, E. H.; Mason, R. Factors Influencing the Oxidation, Reduction, Methylation and Demethylation of Mercury Species in Coastal Waters. *Mar. Chem.* **2007**, *107* (3), 278−294.
(12) Schartup, A. T.; Balcom, P. H.; Soerensen, A. L.; Gosnell, K. J.; Calder, R. S. D.; Mason, R. P.; Sunderland, E. M. Freshwater Discharges Drive High Levels of Methylmercury in Arctic Marine Biota. *Proc. Natl. Acad. Sci. U. S. A.* **2015**, *112* (38), 11789−11794.
(13) Lehnherr, I.; St Louis, V. L.; Hintelmann, H.; Kirk, J. L. Methylation of Inorganic Mercury in Polar Marine Waters. *Nat. Geosci.* **2011**, *4* (5), 298−302.
(14) Sharif, A.; Monperrus, M.; Tessier, E.; Bouchet, S.; Pinaly, H.; Rodriguez-Gonzalez, P.; Maron, P.; Amouroux, D. Fate of Mercury Species in the Coastal Plume of the Adour River Estuary (Bay of Biscay, Sw France). *Sci. Total Environ.* **2014**, *496*, 701−713.
(15) Heimburger, L. E.; Cossa, D.; Marty, J. C.; Migon, C.; Averty, B.; Dufour, A.; Ras, J. Methyl Mercury Distributions in Relation to the Presence of Nano- and Picophytoplankton in an Oceanic Water Column (Ligurian Sea, North-Western Mediterranean). *Geochim. Cosmochim. Acta* **2010**, *74* (19), 5549−5559.
(16) Sunderland, E. M.; Krabbenhoft, D. P.; Moreau, J. W.; Strode, S. A.; Landing, W. M. Mercury Sources, Distribution, and Bioavailability in the North Pacific Ocean: Insights from Data and Models. *Glob. Biogeochem. Cycles* **2009**, *23*, (Artn Gb2010); DOI 10.1029/2008GB003425.
(17) Gionfriddo, C. M.; Tate, M. T.; Wick, R. R.; Schultz, M. B.; Zemla, A.; Thelen, M. P.; Schofield, R.; Krabbenhoft, D. P.; Holt, K. E.; Moreau, J. W. Microbial Mercury Methylation in Antarctic Sea Ice. *Nat. Microbiol.* **2016**, *1*, 16127.
(18) Podar, M.; Gilmour, C. C.; Brandt, C. C.; Soren, A.; Brown, S. D.; Crable, B. R.; Palumbo, A. V.; Somenahally, A. C.; Elias, D. A. Global Prevalence and Distribution of Genes and Microorganisms Involved in Mercury Methylation. *Science adv.* **2015**, *1* (9), e1500675.
(19) Beutel, M.; Dent, S.; Reed, B.; Marshall, P.; Gebremariam, S.; Moore, B.; Cross, B.; Gantzer, P.; Shallenberger, E. Effects of Hypolimnetic Oxygen Addition on Mercury Bioaccumulation in Twin Lakes, Washington, USA. *Sci. Total Environ.* **2014**, *496*, 688−700.
(20) Matthews, D. A.; Babcock, D. B.; Nolan, J. G.; Prestigiacomo, A. R.; Effler, S. W.; Driscoll, C. T.; Todorova, S. G.; Kuhr, K. M. Whole-Lake Nitrate Addition for Control of Methylmercury in Mercury-Contaminated Onondaga Lake, NY. *Environ. Res.* **2013**, *125*, 52−60.
(21) Eckley, C. S.; Hintelmann, H. Determination of Mercury Methylation Potentials in the Water Column of Lakes across Canada. *Sci. Total Environ.* **2006**, *368* (1), 111−125.
(22) Achá, D.; Hintelmann, H.; Pabón, C. A. Sulfate-Reducing Bacteria and Mercury Methylation in the Water Column of the Lake 658 of the Experimental Lake Area. *Geomicrobiol. J.* **2012**, *29* (7), 667−674.
(23) Lamborg, C. H.; Yiğiterhan, O.; Fitzgerald, W. F.; Balcom, P. H.; Hammerschmidt, C. R.; Murray, J. Vertical Distribution of Mercury Species at Two Sites in the Western Black Sea. *Mar. Chem.* **2008**, *111* (1), 77−89.
(24) Myrberg, K.; Lehmann, A. Topography, Hydrography, Circulation and Modelling of the Baltic Sea. In *Preventive Methods for Coastal Protection*; Springer: New York, 2013; pp 31−64.
(25) *Eutrophication Status of the Baltic Sea 2007−2011—a Concise Thematic Assessment. Baltic Sea Environmental Proceedings No. 143*, HELCOM, 2014; http://www.helcom.fi/lists/publications/bsep143.pdf.
(26) Reissmann, J. H.; Burchard, H.; Feistel, R.; Hagen, E.; Lass, H. U.; Mohrholz, V.; Nausch, G.; Umlauf, L.; Wieczorek, G. Vertical Mixing in the Baltic Sea and Consequences for Eutrophication−a Review. *Prog. Oceanogr.* **2009**, *82* (1), 47−80.
(27) Carstensen, J.; Andersen, J. H.; Gustafsson, B. G.; Conley, D. J. Deoxygenation of the Baltic Sea During the Last Century. *Proc. Natl. Acad. Sci. U. S. A.* **2014**, *111* (15), 5628−5633.
(28) Gustafsson, B. G.; Schenk, F.; Blenckner, T.; Eilola, K.; Meier, H. E. M.; Muller-Karulis, B.; Neumann, T.; Ruoho-Airola, T.; Savchuk, O. P.; Zorita, E. Reconstructing the Development of Baltic Sea Eutrophication 1850−2006. *Ambio* **2012**, *41*, 534−548.
(29) Vahtera, E.; Conley, D. J.; Gustafsson, B. G.; Kuosa, H.; Pitkänen, H.; Savchuk, O. P.; Tamminen, T.; Viitasalo, M.; Voss, M.; Wasmund, N. Internal Ecosystem Feedbacks Enhance Nitrogen-Fixing Cyanobacteria Blooms and Complicate Management in the Baltic Sea. *Ambio* **2007**, *36* (2), 186−194.
(30) Savchuk, O. P.; Gustafsson, B. G.; Muller-Karulis, B. *Baltsem—A Marine Model for Decision Support within the Baltic Sea Region (Technical Report No. 7), Bni Technical Report Series*, 2012.
(31) Gustafsson, B. G. Time-Dependent Modeling of the Baltic Entrance Area. 1. Quantification of Circulation and Residence Times in the Kattegat and the Straits of the Baltic Sill. *Estuaries* **2000**, *23* (2), 231−252.
(32) Gustafsson, E.; Deutsch, B.; Gustafsson, B. G.; Humborg, C.; Morth, C. M. Carbon Cycling in the Baltic Sea - the Fate of Allochthonous Organic Carbon and Its Impact on Air-Sea Co2 Exchange. *J. Mar. Sys.* **2014**, *129*, 289−302.
(33) Saniewska, D.; Beldowska, M.; Beldowski, J.; Jedruch, A.; Saniewski, M.; Falkowska, L. Mercury Loads into the Sea Associated with Extreme Flood. *Environ. Pollut.* **2014**, *191*, 93−100.
(34) Kulinski, K.; Pempkowiak, J. The Carbon Budget of the Baltic Sea. *Biogeosciences* **2011**, *8* (11), 3219−3230.
(35) SLU, Institutionen För Vatten Och Miljö: Flodmynningar (1965−2013), database: http://info1.ma.slu.se/ma/www_ma.acgi$ProjectP?ID=Intro&P=FLODMYNN.
(36) Kocman, D.; Horvat, M.; Pirrone, N.; Cinnirella, S. Contribution of Contaminated Sites to the Global Mercury Budget. *Environ. Res.* **2013**, *125*, 160−170.
(37) *The Fifth Baltic Sea Pollution Load Compilation (Plc-5). Balt. Sea Environ. Proc. No. 128*, HELCOM 2011; http://Helcom.Fi/Lists/Publications/Bsep128.Pdf.
(38) Saniewska, D.; Beldowska, M.; Beldowski, J.; Saniewski, M.; Szubska, M.; Romanowski, A.; Falkowska, L. The Impact of Land Use and Season on the Riverine Transport of Mercury into the Marine Coastal Zone. *Environ. Monit. Assess.* **2014**, *186* (11), 7593−7604.
(39) Zhang, Y.; Jacob, D. J.; Dutkiewicz, S.; Amos, H. M.; Sunderland, E. M. Biogeochemical Drivers of the Fate of Riverine Mercury Disharged to the Global and Arctic Oceans. *Glob. Biogeochem. Cy.* **2015**, *29*, 854−864.

DOI: 10.1021/acs.est.6b02717
Environ. Sci. Technol. XXXX, XXX, XXX−XXX

(40) Walsh, J.; Nittrouer, C. Understanding Fine-Grained River-Sediment Dispersal on Continental Margins. *Mar. Geol.* **2009**, *263* (1), 34−45.
(41) *Atmospheric Deposition of Heavy Metals on the Baltic Sea: Baltic Sea Environment Fact Sheet 2014;* http://helcom.fi/baltic-sea-trends/environment-fact-sheets/hazardous-substances/atmospheric-deposition-of-heavy-metals-on-the-baltic-sea/ (accessed March 2015).
(42) Bartnicki, J.; Gusev, A.; Aas, W.; Valiyaveetil, S. *Atmospheric Supply of Nitrogen, Lead, Cadmium, Mercury and Dioxins/Furans to the Baltic Sea in 2010*, EMEP Centres Joint Report for HELCOM, 2012.
(43) Rose, N. L.; Munthe, J.; McCartney, A. Winter Peaks of Methylmercury in Deposition to a Remote Scottish Mountain Lake. *Chemosphere* **2013**, *90* (2), 805−811.
(44) Weiss-Penzias, P. S.; Ortiz, C.; Acosta, R. P.; Heim, W.; Ryan, J. P.; Fernandez, D.; Collett, J. L.; Flegal, A. R. Total and Monomethyl Mercury in Fog Water from the Central California Coast. *Geophys. Res. Lett.* **2012**, *39* (3), L03804.
(45) Munthe, J.; Hultberg, H.; Iverfeldt, Å. Mechanisms of Deposition of Methylmercury and Mercury to Coniferous Forests. In *Mercury as a Global Pollutant*; Springer: New York, 1995; pp 363−371.
(46) Pohl, C.; Hennings, U. *Trace Metal Concentrations and Trends in Baltic Surface and Deep Waters. Helcom Baltic Sea Environment Fact Sheet 2009;* http://Helcom.Fi/Baltic-Sea-Trends/Environment-Fact-Sheets/Hazardous-Substances/Trace-Metal-Concentrations-and-Trends-in-Baltic-Surface-and-Deep-Waters/ (accessed March 2016).
(47) Kuss, J.; Schneider, B. Variability of the Gaseous Elemental Mercury Sea-Air Flux of the Baltic Sea. *Environ. Sci. Technol.* **2007**, *41* (23), 8018−8023.
(48) Wangberg, I.; Schmolke, S.; Schager, P.; Munthe, J.; Ebinghaus, R.; Iverfeldt, A. Estimates of Air-Sea Exchange of Mercury in the Baltic Sea. *Atmos. Environ.* **2001**, *35* (32), 5477−5484.
(49) Horvat, M.; Kotnik, J.; Logar, M.; Fajon, V.; Zvonaric, T.; Pirrone, N. Speciation of Mercury in Surface and Deep-Sea Waters in the Mediterranean Sea. *Atmos. Environ.* **2003**, *37*, 93−108.
(50) Borell, M.; Wik-Persson, M.; Åberg, L. *Miljörapport 2007, Rönnskärsverken Och Rönnskärs Hamn, RMS 8021,* 2008 (www.boliden.com/sv/).
(51) Leipe, T.; Moros, M.; Kotilainen, A.; Vallius, H.; Kabel, K.; Endler, M.; Kowalski, N. Mercury in Baltic Sea Sediments—Natural Background and Anthropogenic Impact. *Chem. Erde* **2013**, *73* (3), 249−259.
(52) Horowitz, H. M.; Jacob, D. J.; Amos, H. M.; Streets, D. G.; Sunderland, E. M. Historical Mercury Releases from Commercial Products: Global Environmental Implications. *Environ. Sci. Technol.* **2014**, *48* (17), 10242−10250.
(53) Fitzgerald, W. F.; Lamborg, C. H.; Hammerschmidt, C. R. Marine Biogeochemical Cycling of Mercury. *Chem. Rev.* **2007**, *107* (2), 641−662.
(54) Schartup, A. T.; Ndu, U. C.; Balcom, P. H.; Mason, R. P.; Sunderland, E. M. Contrasting Effects of Marine and Terrestrially Derived Dissolved Organic Matter on Mercury Speciation and Bioavailability Inseawater. *Environ. Sci. Technol.* **2015**, *49* (10), 5965−5972.
(55) Soerensen, A. L.; Sunderland, E. M.; Holmes, C. D.; Jacob, D. J.; Yantosca, R. M.; Skov, H.; Christensen, J. H.; Strode, S. A.; Mason, R. P. An Improved Global Model for Air-Sea Exchange of Mercury: High Concentrations over the North Atlantic. *Environ. Sci. Technol.* **2010**, *44* (22), 8574−8580.
(56) Deutsch, B.; Alling, V.; Humborg, C.; Korth, F.; Mörth, C. Tracing Inputs of Terrestrial High Molecular Weight Dissolved Organic Matter within the Baltic Sea Ecosystem. *Biogeosciences* **2012**, *9* (11), 4465−4475.
(57) Soerensen, A. L.; Mason, R. P.; Balcom, P. H.; Sunderland, E. M. Drivers of Surface Ocean Mercury Concentrations and Air-Sea Exchange in the West Atlantic Ocean. *Environ. Sci. Technol.* **2013**, *47*, 7757−7765.
(58) Fernandez-Gomez, C.; Drott, A.; Bjorn, E.; Diez, S.; Bayona, J. M.; Tesfalidet, S.; Lindfors, A.; Skyllberg, U. Towards Universal Wavelength-Specific Photodegradation Rate Constants for Methyl Mercury in Humic Waters, Exemplified by a Boreal Lake-Wetland Gradient. *Environ. Sci. Technol.* **2013**, *47* (12), 6279−6287.
(59) Zhang, T.; Hsu-Kim, H. Photolytic Degradation of Methylmercury Enhanced by Binding to Natural Organic Ligands. *Nat. Geosci.* **2010**, *3* (7), 473−476.
(60) Kim, M.-K.; Won, A.-Y.; Zoh, K.-D. The Production of Dissolved Gaseous Mercury from Methylmercury Photodegradation at Different Salinity. *Desalin. Water Treat.* **2016**, *57* (2), 610−619.
(61) Black, F. J.; Poulin, B. A.; Flegal, A. R. Factors Controlling the Abiotic Photo-Degradation of Monomethylmercury in Surface Waters. *Geochim. Cosmochim. Acta* **2012**, *84*, 492−507.
(62) Jonsson, S.; Skyllberg, U.; Nilsson, M. B.; Lundberg, E.; Andersson, A.; Bjorn, E. Differentiated Availability of Geochemical Mercury Pools Controls Methylmercury Levels in Estuarine Sediment and Biota. *Nat. Commun.* **2014**, *5*; 462410.1038/ncomms5624.
(63) Soerensen, A. L.; Jacob, D. J.; Schartup, A.; Fisher, J. A.; Lehnherr, I.; St Louis, V. L.; Heimburger, L. E.; Sonke, J.; Krabbenhoft, D. P.; Sunderland, E. M. A Mass Budget for Mercury and Methylmercury in the Arctic Ocean. *Glob. Biogeochem. Cy.* **2016**, *30*, 560−575.
(64) Hollweg, T. A.; Gilmour, C. C.; Mason, R. P. Mercury and Methylmercury Cycling in Sediments of the Mid-Atlantic Continental Shelf and Slope. *Limnol. Oceanogr.* **2010**, *55* (6), 2703−2722.
(65) Schartup, A. T.; Mason, R. P.; Balcom, P. H.; Hollweg, T. A.; Chen, C. Y. Methylmercury Production in Estuarine Sediments: Role of Organic Matter. *Environ. Sci. Technol.* **2013**, *47* (2), 695−700.
(66) Beldowski, J.; Miotk, M.; Beldowska, M.; Pempkowiak, J. Total, Methyl and Organic Mercury in Sediments of the Southern Baltic Sea. *Mar. Pollut. Bull.* **2014**, *87* (1−2), 388−395.
(67) Dryden, C. L.; Gordon, A. S.; Donat, J. R. Seasonal Survey of Copper-Complexing Ligands and Thiol Compounds in a Heavily Utilized, Urban Estuary: Elizabeth River, Virginia. *Mar. Chem.* **2007**, *103* (3), 276−288.
(68) Skyllberg, U. Competition among Thiols and Inorganic Sulfides and Polysulfides for Hg and Mehg in Wetland Soils and Sediments under Suboxic Conditions: Illumination of Controversies and Implications for MeHg Net Production. *J. Geophys. Res.-Biogeo.* **2008**, *113*, (G2).10.1029/2008JG000745
(69) Sunderland, E. M.; Dalziel, J.; Heyes, A.; Branfireun, B. A.; Krabbenhoft, D. P.; Gobas, F. A. P. C. Response of a Macrotidal Estuary to Changes in Anthropogenic Mercury Loading between 1850 and 2000. *Environ. Sci. Technol.* **2010**, *44* (5), 1698−1704.
(70) Leipe, T.; Tauber, F.; Vallius, H.; Virtasalo, J.; Uścinowicz, S.; Kowalski, N.; Hille, S.; Lindgren, S.; Myllyvirta, T. Particulate Organic Carbon (Poc) in Surface Sediments of the Baltic Sea. *Geo-Mar. Lett.* **2011**, *31* (3), 175−188.
(71) Nightingale, P. D.; Malin, G.; Law, C. S.; Watson, A. J.; Liss, P. S.; Liddicoat, M. I.; Boutin, J.; Upstill-Goddard, R. C. In Situ Evaluation of Air-Sea Gas Exchange Parameterizations Using Novel Conservative and Volatile Tracers. *Glob. Biogeochem. Cy.* **2000**, *14* (1), 373−387.
(72) Baya, P. A.; Gosselin, M.; Lehnherr, I.; St Louis, V. L.; Hintelmann, H. Determination of Monomethylmercury and Dimethylmercury in the Arctic Marine Boundary Layer. *Environ. Sci. Technol.* **2015**, *49* (1), 223−232.
(73) Hansson, M.; Andersson, L.; Axe, P. *Areal Extent and Volume of Anoxia and Hypoxia in the Baltic Sea, 1960−2011;* SMHI, report oceanography No. 42, 2011; www.smhi.se/polopoly_fs/1.19219!Oxygen_timeseries_1960_2010_20111219.pdf.
(74) Alpers, C. N.; Fleck, J. A.; Marvin-DiPasquale, M.; Stricker, C. A.; Stephenson, M.; Taylor, H. E. Mercury Cycling in Agricultural and Managed Wetlands, Yolo Bypass, California: Spatial and Seasonal Variations in Water Quality. *Sci. Total Environ.* **2014**, *484*, 276−287.
(75) Fleming, E. J.; Mack, E. E.; Green, P. G.; Nelson, D. C. Mercury Methylation from Unexpected Sources: Molybdate-Inhibited Freshwater Sediments and an Iron-Reducing Bacterium. *Appl. Environ. Microb.* **2006**, *72* (1), 457−464.

DOI: 10.1021/acs.est.6b02717
Environ. Sci. Technol. XXXX, XXX, XXX−XXX

(76) Chen, C. Y.; Driscoll, C. T.; Lambert, K. F.; Mason, R. P.; Rardin, L. R.; Serrell, N.; Sunderland, E. M. Marine Mercury Fate: From Sources to Seafood Consumers. *Environ. Res.* **2012**, *119*, 1−2.
(77) Jakobs, G.; Holtermann, P.; Berndmeyer, C.; Rehder, G.; Blumenberg, M.; Jost, G.; Nausch, G.; Schmale, O. Seasonal and Spatial Methane Dynamics in the Water Column of the Central Baltic Sea (Gotland Sea). *Cont. Shelf Res.* **2014**, *91*, 12−25.
(78) Omstedt, A.; Elken, J.; Lehmann, A.; Leppäranta, M.; Meier, H.; Myrberg, K.; Rutgersson, A. Progress in Physical Oceanography of the Baltic Sea During the 2003−2014 Period. *Prog. Oceanogr.* **2014**, *128*, 139−171.
(79) Sellner, K.; Olson, M.; Olli, K. Copepod Interactions with Toxic and Non-Toxic Cyanobacteria from the Gulf of Finland. *Phycologia* **1996**, *35* (6S), 177−182.
(80) Karlson, A. M.; Duberg, J.; Motwani, N. H.; Hogfors, H.; Klawonn, I.; Ploug, H.; Svedén, J. B.; Garbaras, A.; Sundelin, B.; Hajdu, S. Nitrogen Fixation by Cyanobacteria Stimulates Production in Baltic Food Webs. *Ambio* **2015**, *44* (S3), 413−426.
(81) Lesutienė, J.; Bukaveckas, P. A.; Gasiunaitė, Z. R.; Pilkaitytė, R.; Razinkovas-Baziukas, A. Tracing the Isotopic Signal of a Cyanobacteria Bloom through the Food Web of a Baltic Sea Coastal Lagoon. *Estuarine, Coastal Shelf Sci.* **2014**, *138*, 47−56.

DOI: 10.1021/acs.est.6b02717
Environ. Sci. Technol. XXXX, XXX, XXX−XXX